Journal of
Nanoscience and Nanotechnology
Vol. 11, 6044–6048, 2011

RESEARCH ARTICLE

Organic Memory Capacitor Device Fabricated with Ag Nanoparticles

Yo-Han Kim[1], Sung Mok Jung[1], Quanli Hu[2], Yong-Sang Kim[2], Tae-Sik Yoon[2,*], and Hyun Ho Lee[1,*]

[1] *Department of Chemical Engineering, Myongji University, Yongin 449-728, Republic of Korea*
[2] *Department of Nano Science and Engineering, Myongji University, Yongin 449-728, Republic of Korea*

In this study, it is demonstrated that an organic memory structure using pentacene and citrate-stabilized silver nanoparticles (Ag NPs) as charge storage elements on dielectric SiO_2 layer and silicon substrate. The Ag NPs were synthesized by thermal reduction method of silver trifluoroacetate with oleic acid. The synthesized Ag NPs were analyzed with high resolution transmission electron microscopy (HRTEM) and selected area electron diffraction (SAED) for their crystalline structure. The capacitance versus voltage (*C–V*) curves obtained for the Ag NPs embedded capacitor exhibited flat-band voltage shifts, which demonstrated the presence of charge storages. The citrate-capping of the Ag NPs was confirmed by ultraviolet-visible (UV-VIS) and Fourier transformed infrared (FTIR) spectroscopy. With voltage sweeping of +/−7 V, a hysteresis loop having flatband voltage shift of 7.1 V was obtained. The hysteresis loop showed a counter-clockwise direction. In addition, electrical performance test for charge storage showed more than 10,000 second charge retention time. The device with Ag NPs can be applied to an organic memory device for flexible electronics.

Keywords: Organic Memory Capacitor, Ag Nanoparticles.

1. INTRODUCTION

Recently, memory cell structures consisting of semiconductor or metal nanoparticles embedded inside of insulators have received considerable attentions due to their low operation voltage, fast write/erase speeds, and better endurance compared with conventional flash memory devices.[1–5] Particularly, metal-insulator-semiconductor (MIS) capacitors with nanoparticles (NPs) (or nanocrystal) have attracted much interests both for new physical phenomena and for potential applications in next generation devices.[3,5–7] Even for silicon-based memory device, to overcome the scaling issue of electronic non-volatile memories, NPs can be an attractive charging element due to its nanoscale size.[5] In addition, NPs memories based on organic materials could have been developed as an alternative solution over silicon-based device for bendable or flexible electronics.[1,3] However, so far, the precise control of NPs to incorporate between gate dielectric layers has been a difficulty for a reliable device fabrication. Therefore, monolayer formations of NPs are of great interests to have uniform charging layer between dielectric layers. Recently, a biomolecular binding method was represented to have a relatively uniform layer comparable to the binding format of electrostatic interaction between the surface-modified NPs' carboxylate(COO^-) of citrate and the SiO_2 surface-modified amine groups(NH_3^+) of APTES.[6,7]

For the materials of the NPs as the charging element, metallic NPs have been frequently reported.[1,3–5] Metals such as gold (Au) and platinum (Pt) are not easily oxidized. As an alternative to semiconductor nanoparticles, metallic NPs, for example, the Au NPs have been widely investigated.[1,3] The metal NPs having large work-function have the potential to enhance the retention characteristic without sacrificing injection efficiency.[4] Therefore, the metallic NPs have the potential for more versatile engineering of energy barriers that would allow improved data retention for memory devices operating at low voltages.[3–6] Very recently, silver (Ag) NPs layer was reported to be embedded between two pentacene layers of organic field-effect transistor to have memory characteristics.[8] The Ag NPs layer was formed by thermal evaporation having a high areal density of NPs on pentacene and a huge memory window of 90 V having a high threshold voltage

*Authors to whom correspondence should be addressed.

 1533-4880/2011/11/6044/005 doi:10.1166/jnn.2011.4370

shift.[8] In this study, metallic Ag NPs were synthesized in organic thermal reduction method and adopted in memody device.[9, 10] The synthesized Ag NPs were uniformly distributed in size without any size-selection method. The Ag NPs were processed to be used as charging elements in metal-pentacene-insulator-silicon (MPIS) capacitor structure. The synthesized Ag NPs were capped by citrate molecules, which can bind to amine group terminals of 3-aminopropyl-triethoxysilane (APTES) by electrostatic force.[1, 6] Approaches for Ag NPs formation process are addressed and corresponding memory device performances are also discussed.

2. EXPERIMENTAL DETAILS

The Ag NPs are synthesized by the reduction of silver trifluoroacetate in the presence of oleic acid in the isoamyl ether. Silver trifluoroacetate (0.27 g), oleic acid (99%, 1.14 ml), and isoamyl ether (20 mL) were mixed in a three-neck round-bottom flask under a gentle flow of N_2 and stirred vigorously using a magnetic stirrer. The reaction flask was heated to 160 °C with a heating rate of 2 °C min^{-1}. After keeping the solution at 160 °C for 90 min, the solution was cooled to room temperature. The synthesized particles were precipitated out from the solution mixture by adding ethanol and separated by centrifugation. The yellow-brown supernatant was discarded and the brown precipitates, silver (Ag) particles with a diameter of 9∼10 nm, were dispersed in hexane. The prepared Ag NPs were analyzed by a high resolution transmission electron microscopy (HRTEM). A carbon grid(Type-A, 400 mesh, Cu, Ted Pella) was used to have TEM image of the Ag NPs drop-casted and dried at room temperature. The Ag NPs was suspended in hexane without capping of citrate. The TEM image of the Ag NPs and selected area electron diffraction(SAED) were obtained by JEOL JEM 2100F microscope at an accelerating voltage of 200 keV. SiO_2 thermally grown to 10 nm on heavily doped *P*-type Si substrate [100] was a gate insulator. APTES (99%, Aldrich Chemistry) was deposited by dip-coating at 3.0 vol% solution with ethanol in order to immobilize amide group on SiO_2 surface. Ag NPs were capped by citric acid (diluted in DI water) with mixing and incubation. The capped NPs were centrifugated to filter remained Ag NPs that were not coated by citric acid. For more detailed filtration procedures are illustrated in Ref. [6]. The capped Ag NPs was confirmed by FTIR (JASCO FT/IR460). The device was immersed in the solution of citrate capped Ag NPs solution. For removing the odd Ag NPs unbound on the surface of APTES, then device was rinsed in DI water for 12 hours. Pentacene active layer and gold electrode 0.5 mm diameter were deposited by thermal evaporator with 60 nm of thickness and 100 nm of thickness, respectively. *C–V* performance was measured by HP Agilent 4284 A at 100 kHz and 1 MHz of frequency. Retention test was performed by biasing 8 V to top electrode for 20 s and then *C–V* recoveries were measured with time.

3. RESULTS AND DISCUSSION

Figure 1 shows (a) a HRTEM image of the synthesized Ag NPs, and (b) a SAED pattern of the Ag NPs. As shown in Figure 1, there were many Ag NPs that were well dispersed. In addtion, there were no nanowires or nanorods as confirmed in the TEM image and most of Ag NPs were spherical. The shape and size distribution in the synthesis of Ag NPs are closely related to solvent, surfactant, and precursor.[9–11] It is found that the precursor of silver trifluoroacetate rather than silver nitrate and the surfacetant of oleic acid in this study were attributed to having a narrow sized spherical distribution of the Ag NPs.[9] The size of the Ag NPs is ranged within 9∼10 nm in diameter. From the TEM image in Figure 1(a), it is noticed that the Ag NPs are in polycrystalline nature with inhomogeneous contrast

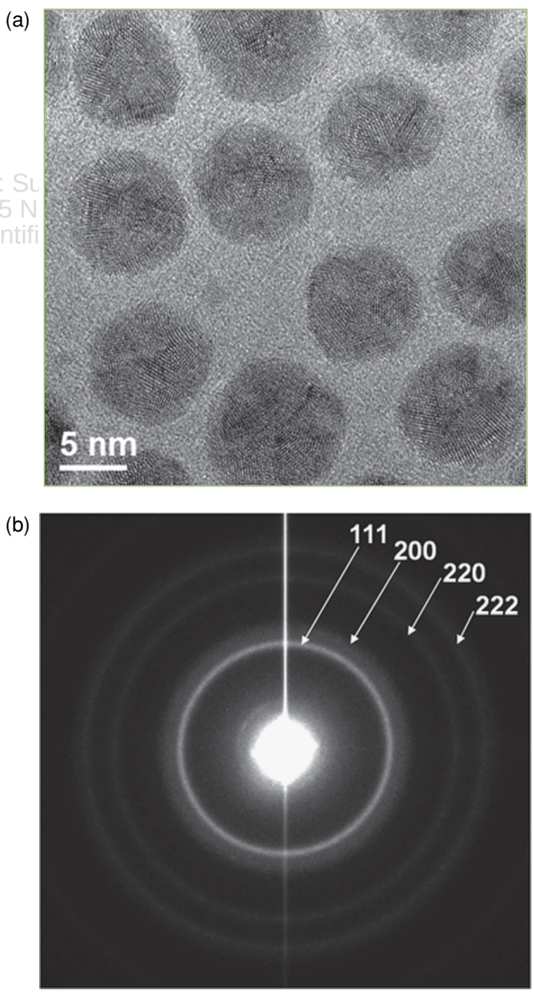

Fig. 1. (a) a HRTEM image of the Ag NPs, and (b) a SAED pattern of the Ag NPs.

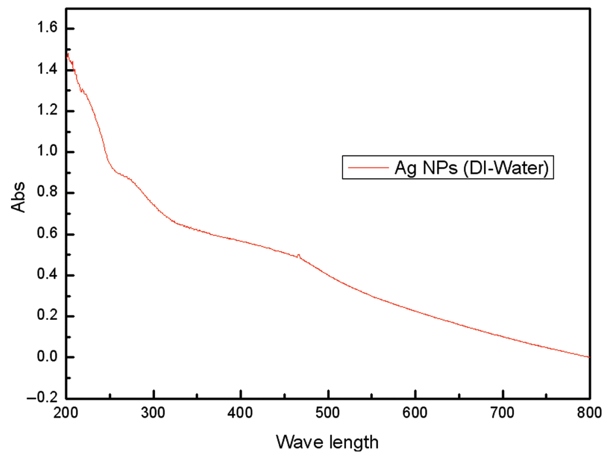

Fig. 2. UV-VIS spectra of citrate capped Ag NPs in DI water.

within a single nanoparticle. Unlike previous report, residual Ag NPs less than ~2 nm were not detected in this study due to usage of centrifugational process and size exclusive filtration process for citrate capping. We used SAED to characterize the crystalline structures of the NPs. The diffraction can be indexed to the (111), (200), (220), and (222) planes of face-centered cubic(fcc) silver, respectively. The ED rings were relatively broad due to the nature of polycrystalline structures as proven in the TEM image.[9,11]

Figure 2 shows the result of UV-VIS absorption graph of citrate-capped Ag NPs. For the Ag NPs dispersed in hexane after their synthesis, UV-VIS absorption peak in the wavelength nearby 417 nm was reported to be detected.[9] It is known a characteristic peak for surface plasmon band from Ag NPs. However, for citrate-capped Ag NPs, absorption peak near 465.5 nm was detected as shown in Figure 2, which is not clearly characterized.

Figure 3 shows a schematic structure of memory device by Ag NPs. The MPIS structure has several advantages over the capacitor devices without using pentacene. First, the gold electrode and pentacene layer are known as a good match for charge carrier injection. Second, pentacene layer was adopted as thick as 60 nm, where it can act as a semiconductor as well as a dielectric layer.[3] The good carrier injection through the pentacene is adopted to have an efficient pathway for the charge trapping injected from the top gate electrode. The semiconducting nature of the

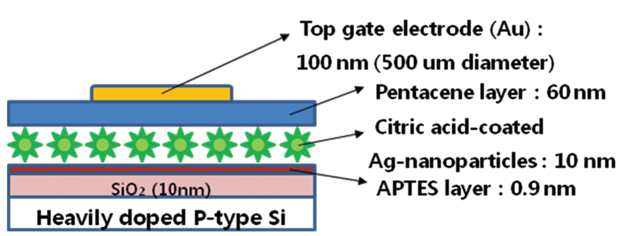

Fig. 3. Structure of MPIS memory device with Ag NPs intervened between dielectric and pentacene.

pentacene can be further utilized to fabricate a field-effect transistor as reported in the previous literature.[8] In a separate experiment, a soluble semiconductor layer, such as poly 3-hexylthiophene (P3HT), was introduced instead of pentacene evaporation by a spin coating. However, the bound layer of Ag NPs was deteriorated by shear stress originated from the spin coating process (data not shown). Therefore, in order to sustain the layer structure of the charging NPs, a moderate film formation method of the pentacene evaporation or a strong binding method rather than the electrostatic interaction is inevitable.

During the capping process of Ag NPs with the citrate, bindings of citrate on the Ag NPs could be confirmed by FTIR. Figure 4 shows the FTIR spectra of the Ag NPs without capping and the Ag NPs with citrate capping. In Figure 4, peaks at 1150 cm^{-1}, 1210 cm^{-1}, 1450 cm^{-1}, 2844 cm^{-1}, and 2920 cm^{-1} are observed as methyl groups, which are from methyl groups in hexane and citrate.[12] However, only in the spectra of citrate-capped Ag NPs, additional peaks near 1710 cm^{-1} are detected, which correspond C═O bond from citrate. If surfactant or capping molecules are anchored to Ag NPs, the TFIR peaks are often shifted from the original peak's positions.[10,11] It is why the C═O bond peak from carboxylic group (~1725 cm^{-1}) appeared in a shifted position (~1710 cm^{-1}) as shown in Figure 4. The difference in the FTIR spectra between the Ag NPs with and without capping proves that the binding of citrate on the Ag NPs was successfully formed.

Figure 5 shows the *C–V* characteristics of the device at 100 kHz frequency measurement under different voltage sweep range with Ag NPs. As shown in Figure 5, increase of voltage sweeping range from +/−3 V to +/−7 V increases the flatband voltage shift (ΔV_{FB}). The ΔV_{FB} for +/− 3 V range measured as 1.2 V was increased to 7.1 V for +/− 7 V range. The hysteresis loops are measured in counter-clockwise direction. The counter-clockwise characteristics come from a mechanism that electrons were

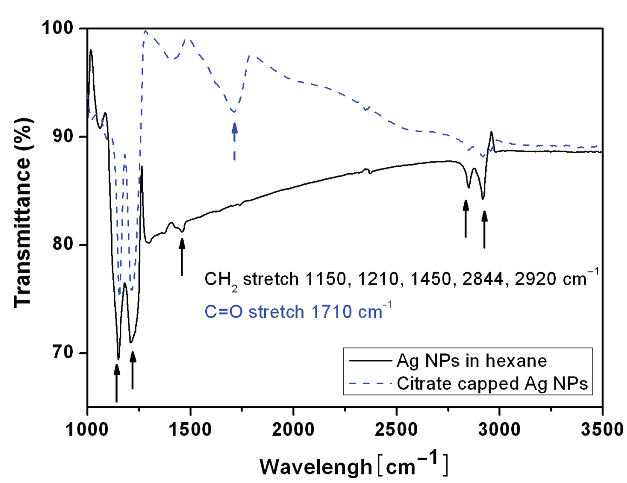

Fig. 4. FTIR spectra of Ag NPs in hexane and citrate capped Ag NPs in DI water.

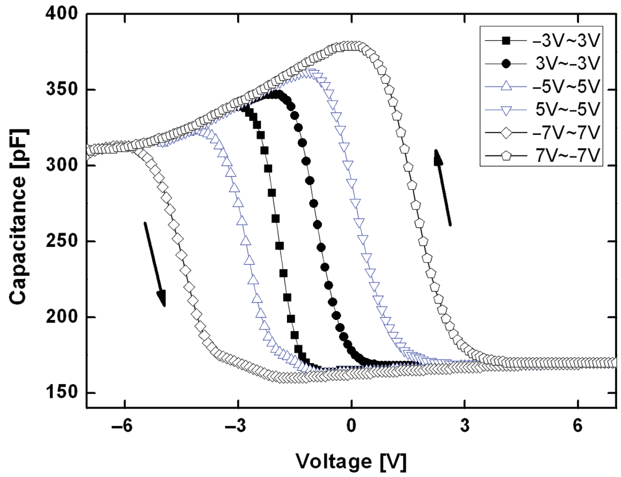

Fig. 5. *C–V* characteristic at 100 kHz.

injected through the thin oxide in the depletion region of *p*-type Si. It again indicates that when applying the negative voltage at the top gate electrode, the holes could be injected from the *p*-type Si into the Au NPs. As sweep range was increased to (+/−)7 V, the V_{FB} was shifted negatively or positively depending on the forward or backward sweep direction unlike the cases of (+/−)3 V sweep. These results indicate that the charge tramsport from *p*-type Si is more efficient than the transport from the top electrode. For metal nanocrystal embedded cMOS devices, the thicknesses of the tunnel oxide have been reported to range 4 nm to 8 nm.[13, 14] It is suggested that leaky oxide formation at low oxidational condition or at low temperature may be one of the explanations.[3, 7] As shown in Figure 5, it is shown significant decreases in accumulation capacitance as the voltage into accumulation is increased. It is known to be originated from the ultrathin dielectric layer for capacitance measurement.[15] When a 30 nm thick SiO_2 was used to fabricate the MPIS device, no decreases in accumulation capacitance were detected.[7] The decreases are more significant with a change of frequency. For example, *C–V* behaviour at 1 MHz measurement shows more drastic decreases of capacitance at the accumulation. The origin of the decreased capacitance behavior is considered from both the leakage conductance of the thin SiO_2 dielectric and the resistance of the Si substrate below the oxide.[15]

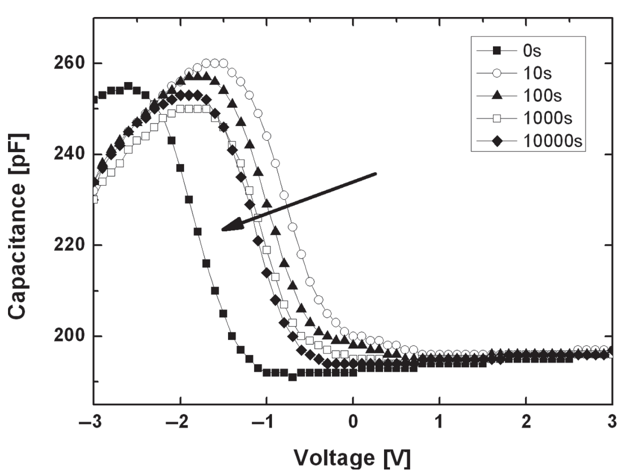

Fig. 6. Retention characteristic of *C–V* measurement at 1 MHz.

Figure 6 shows the results of retention test for the charge storage of the Ag NPs measured at 1 MHz frequency. The test was performed by biasing −8 V for 10 s at first, then, *C–V* measurements were executed sequentially after 0 s, 10 s, 100 s, 1,000 s, and 10,000 s after the bias. It was measured that the stored charge was retained upto 10,000 s. However, after 10,000 s, the *C–V* curves were converged into the 10,000 s *C–V* curve which represent for an original *C–V* behavior without the bias.

4. CONCLUSIONS

In summary, the fabrication of organic memory device using Ag NPs has been demonstrated. The sweeping *C–V* characteristics of the device were shown to exhibit hysteresis, which indicates net charge trapping effects in the Ag NPs. In the *C–V* curves, the hysteresis loops are formed in a counter-clockwise direction. These observations signify the injection and subsequent transfer of electrons stored in the Ag NPs. In addition, flatband voltage shift increases with increase of sweepting voltage range with the organic Ag NPs memory device. Electrical performance test for the charge storage shows 10,000 second retention time.

Acknowledgments: This work is financially supported by the Ministry of Knowledge Economy (MKE) of Korean Government and Korea Institute for Advancement in Technology (KIAT) through the Workforce Development Program in Strategic Technology.

References and Notes

1. W. L. Leong, P. S. Lee, and S. G. Mhaisalkar, *Appl. Phys. Lett.* 90, 042906 (**2007**).
2. J. Y. Yang, J. H. Kim, J. S. Lee, S. K. Min, H. J. Kim, K. L. Wang, and J. P. Hong, *Ultramicro.* 108, 1215 (**2008**).
3. M. F. Mabrook, C. Pearson, D. Kolb, D. A. Zeze, and M. C. Petty, *Organ. Electron.* 9, 816 (**2008**).
4. B. Park, K. Cho, J. Yun, Y.-S. Koo, J.-H. Lee, and S. Kim, *J. Nanosci. Nanotechnol.* 8, 1 (**2008**).
5. B. Park, K. Cho, Y.-S. Koo, and S. Kim, *Curr. Appl. Phys.* 9, 1334 (**2009**).
6. H.-J. Kim, S. M. Jung, B.-J. Kim, T.-S. Yoon, Y.-S. Kim, and H. H. Lee, *J. Ind. Eng. Chem.* 16, 848 (**2010**).
7. S. M. Jung, H.-J. Kim, B.-J. Kim, T.-S. Yoon, Y.-S. Kim, and H. H. Lee, *Appl. Phys. Lett.* 97, 153302 (**2010**).
8. S. Wang, C.-W. Leung, and P. K. L. Chan, *Organ. Electron.* 11, 990 (**2010**).
9. X. Z. Lin, X. Teng, and H. Yang, *Langmuir* 19, 10081 (**2003**).
10. S. K. Mehta, S. Chaudhary, and M. Gradzielski, *J. Colloid. Inter. Sci.* 343, 447 (**2010**).

11. D. Miranda, V. Sencadas, A. Sanchez-Iglesias, I. Pastoriza-Santos, L. M. Liz-Marzan, J. L. Gomez Ribelles, and S. Lanceros-Mendez, *J. Nanosci. Nanotechnol.* 9, 1 **(2008)**.
12. NIST chemistry webbook, http://webbook.nist.gov/chemistry/, Novemeber **(2010)**.
13. C.-C. Wang, Y.-K. Chiou, C.-H. Chang, J.-Y. Tseng, L.-J. Wu, C.-Y. Chen, and T.-B. Wu, *J. Phys. D: Appl. Phys.* 40, 1673 **(2007)**.
14. P. H. Yeh, L. J. Chen, P. T. Liu, D. Y. Wang, and T. C. Chang, *Electrochem. Acta* 52, 2920 **(2007)**.
15. D. P. Norton, *Solid-St. Electron.* 47, 801 **(2003)**.

Received: 24 June 2010. Accepted: 13 January 2011.

RESEARCH ARTICLE